Biomedical Letters ISSN 2410-955X DOI: https://doi.org/10.47262/BL/9.1.20230503

Research article
2025 | Volume 11 | Issue 2 | Pages 69-79

ARTICLEINFO

Received
May 03, 2025
Revised
July 31, 2025
Accepted
August 05, 2025

***Corresponding Author**
Huma Nawaz

E-mail
humanawaz00@gmail.com

Keywords
RASSF3
Homology modeling
Cancer
Apoptosis
Drug discovery
Bioinformatics

How to Cite
Masood Q, Bibi H, Nawaz H. Comparative modeling and in silico identification of drug target sites in RASSF3. Biomedical Letters 2025; 11(2):69-79.

SCAN ME

Open Access

Comparative modeling and *in silico* identification of drug target sites in RASSF3

Qandeel Masood[1], Haleema Bibi[2], Huma Nawaz[3*]

[1]Department of Biotechnology, University of Okara, Okara, Pakistan
[2]Department of Genomics and Bioinformatics, Cholistan University of Veterinary and Animal Sciences, Bahawalpur, Bahawalpur, Pakistan
[3]Department of Biotechnology, Institute of Biochemistry, Biotechnology and Bioinformatics, The Islamia University of Bahawalpur, Bahawalpur, Pakistan

Abstract

RASSF3 is a gene that encodes a protein with tumor-suppressive properties, primarily by promoting apoptosis and regulating the cell cycle. It plays a significant role in inhibiting cancer progression. In this study, the 3D structure of RASSF3 was predicted using homology modeling. MODELLER (v10.4) and online tools such as I-TASSER, Swiss-Model, and MODWEB were employed for model generation. The structural models were evaluated for accuracy using tools including ERRAT, PROCHECK, and Rampage. The most reliable model, based on validation, was selected for molecular docking studies. Binding pockets of RASSF3 were identified using the CASTp server. Molecular docking was carried out using AutoDock Vina and AutoDock4 to investigate the interaction between RASSF3 and two selected ligands: ANP and GNP. These compounds demonstrated the lowest binding energies of -5.7 and -5.3 Kcal/mol respectively and the highest binding affinities within the top-ranked binding site. Identification of these binding domains and ligand interactions is critical for understanding the functional behavior of RASSF3 and its role in cancer inhibition. The predicted binding pockets and docking results suggest that RASSF3 could serve as a promising target in anticancer drug discovery.

Introduction

Cancer is a malignant tumor and neoplasm that involves irregular cell growth and spreading to other parts of the body [1]. It forms a subset of neoplasms, which are involved in unregulated cell growth and diffuse spreading throughout the body [2]. Cancer development depends on the heterotypic interaction between incipient tumor cells and the normal cells around them. Abnormal cell growth (neoplasia) is the endpoint of the cancer disease [3]. According to Hanahan and Weinberg, six essential alterations can cause malignant tumors: 1) self-sufficiency in growth signals, 2) insensitivity to growth inhibitors, 3) evasion of programmed cell death, 4) limitless replicative potential, 5) sustained angiogenesis, 6) tissue invasion and metastasis [4].

Cancer is a disease of tissue growth regulation. In cancer, the genes involved in regulating tissue growth must be mutated. Mutation refers to changes in the nucleotide sequence of genomic DNA. Mutations inactivate tumor suppressor genes (enhancing cell division and reducing apoptosis), which leads to cancer [5]. There are almost 100 different types of cancer that severely affect humans. Like demographic and lifestyle factors, breast and ovarian cancers are caused by mutations in the *BRCA1* and *BRCA2* genes [2].

Head and neck cell carcinoma is one of the most common types of human cancer, affecting about 500,000 cases worldwide [6]. Head and neck cancer is caused by limitless replicative potential *via* the p53 and retinoblastoma pathways [7]. Normal cells arrest glycolysis in the presence of oxygen and favor ATP production, but cancer cells lose this regulation and perform glycolysis in the absence of O_2, producing lactate [8].

Abnormal splicing of mRNA precursors is a nearly ubiquitous and highly flexible gene checkpoint in humans. This enables cells to create protein isoforms from a single gene, which may have different or even opposing functions. Cancer cells damage this flexibility to produce proteins that promote growth and survival. These isoforms are developmentally regulated and re-expressed in tumors [3]. Chemoprevention is the use of pharmacological or natural agents to inhibit the spread of cancer by blocking DNA damage that leads to carcinogenesis in already-damaged cells [9].

The RASSF family of tumor suppressor genes encodes Ras effector proteins, which mediate the growth-inhibitory function of Ras proteins [10]. The Ras association domain family consists of ten mammalian proteins, RASSF1 to RASSF10. RASSF1 to RASSF6 are called the classical family because they have the SARAH domain at the C-terminal, while RASSF7-10 are called the N-terminal family because they have the RA domain at the N-terminal and lack of SARAH domain. Among RASSF1 to RASSF6, there is a high similarity in RASSF1, RASSF3, and RASSF5, which are believed to have come from a common ancestor [11].

Several members of the RASSF family are inactivated by DNA hypermethylation in cancers. RASSF2 regulates apoptosis through various downstream effectors, such as MST1 and MST2, and can mediate the growth inhibitory properties of K-Ras [12]. RASSF3 (Ras association domain family member 3) is a tumor suppressor gene. Human RASSF3 shows homology to the genomic sequence of mice. RASSF3 is located on chromosome 12q14.1, encodes 238 amino acids, and has a molecular weight of 28.6 kDa. RASSF3 follows a signaling pathway involved in cancer inhibition [13]. The Ras proteins (GTPases) act as molecular switches for signaling pathways. They regulate survival, migration, cytoskeletal dynamism, cell proliferation, differentiation, and growth. Ras proteins cycle between active GTP-bound and inactive GDP-bound states. They activate/inactivate GTP-bound states *via* signal transduction from extracellular growth factors. Guanine nucleotide exchange factors (GEFs) and GTPase-activating proteins (GAPs) regulate the exchange of GTP to GDP on Ras [14].

In breast cancer, the expression of RASSF3 inhibits cell growth by inducing apoptosis. In head and neck cancer, RASSF3 suppresses tumors through p53-dependent apoptosis [15]. Bioinformatics is a multidisciplinary field that combines computational biology, mathematics, molecular biology, and genetics to solve biological problems computationally [16]. Structure prediction techniques like NMR and X-ray crystallography are costly.

Therefore, we can use bioinformatics tools for structure prediction through threading, homology modeling, and *ab initio* approaches. Bioinformatics is a multidisciplinary domain utilized to solve various biological problems through statistics, mathematics, and computational powers [17, 18, 19]. Bioinformatics is used for *in silico* analyses to solve biological problems [20, 21]. Various inhibitors, vaccines, and drug-like compounds have been reported by using computational approaches against diabetes, cancers, viral infections [22], parasitic infections, and neurological diseases [20]. The 3D

structure of RASSF3 has not been reported in the Protein Data Bank (PDB). In this paper, we use computational approaches to predict the 3D structure of RASSF3 and reveal its binding pockets (target sites) against cancer. The target sites of RASSF3 were used for molecular docking with chemically designed ligands.

Materials and Methods

Computational analyses were carried out for the structure prediction of the target protein RASSF3, following approaches reported in previous studies [16]. The amino acid sequence of RASSF3 was retrieved from UniProt [23] database in FASTA format (UniProt ID: Q86WH2). To identify a suitable template for structure prediction, the sequence was subjected to BLASTp and PSI-BLAST against the Protein Data Bank (PDB) [24].

Four suitable templates for RASSF3 were identified. A template with the highest query coverage was selected for structure prediction. Template files in PDB format were downloaded, and both sequence and structural alignments were performed using the UCSF Chimera 1.8 [25]. Based on these alignments, structure prediction was conducted using various servers, including I-TASSER [26], Swiss-Model [27], MODWEB [28], and 3D JigSaw [29], as well as MODELLER 10.4 [30], which was used for comparative modeling with all four templates.

The accuracy of the predicted models was validated using MolProbity [31], ERRAT [32], and Ramachandran plots generated by PROCHECK [33]. The considerable model was selected based on combined evaluation parameters.

Structural refinement was performed using WinCoot [34], where poor rotamers and Ramachandran outliers were corrected. The energy of the refined model was minimized using UCSF Chimera 1.8. The binding pockets (target sites) of RASSF3 were predicted using the CASTp server [35].

Two chemically designed ligands, ANP (Phosphoaminophonic adenylate ester) and GNP (Phosphoaminophonic acid guanylate ester), previously reported in literature, were selected for molecular docking. Ligand structures were optimized and energy minimized using ChemDraw [36].

Molecular docking was performed using AutoDock Vina [37]. The ligands ANP and GNP were docked into the predicted active sites of RASSF3, targeting residues with the highest predicted interaction potential. The docked complexes were visualized and analyzed using UCSF Chimera 1.8.The adopted methodology has been validated and reported [38].

Results and Discussion

The primary objective of this study was to investigate the interaction between RASSF3 and cancer-related pathways through computational analysis. A three-dimensional (3D) structure of RASSF3 was predicted using bioinformatics tools. The study involved structure prediction, identification of potential binding pockets, and molecular docking analysis. The predicted 3D model of RASSF3 demonstrated high structural accuracy, particularly within the identified binding regions, supporting its relevance as a potential drug target.

3D structure of RASSF3 has not yet been reported. The amino acid sequence (238 residues) was retrieved from the UniProt database (accession number: Q86WH2) in FASTA format and subjected to the protein BLAST against the Protein Data Bank (PDB) to identify suitable templates for homology modeling. Four appropriate templates were identified: 3DCC, 4OH8, 4LGD, and 2YMY, with query coverages of 56%, 18%, 18%, and 15%, respectively (**Table 1**).

Table 1: Templates used for RASSF3 homology modeling along with their alignment scores, query coverage, E-values, and sequence identity percentages.

Templates	Max score	Total score	Query coverage	E-value	Identity
3DDC	121	121	56%	2e-34	44%
4OH8	66.6	66.6	18%	1e-14	64%
4LGD	66.2	66.2	18%	1e-14	64%
2YMY	52.8	52.8	15%	1e-09	63%

For structure prediction, the template with the highest query coverage (3DCC) was selected; however, all four templates were used for comparative modeling. The 3D structure of RASSF3 was predicted using MODELLER 10.4 and additional online servers, including Swiss-Model, I-TASSER, and MODWEB. The generated models were evaluated using various validation tools such as MolProbity, ERRAT, and PROCHECK.

Comparative analysis of the predicted models from MODELLER and the online servers was performed and Ramachandran plots and overall quality factor values were analyzed. The most reliable model was selected based on these validation metrics and further visualized.

The predicted 3D model of RASSF3 was evaluated, which analyzes the φ (phi) and ψ (psi) backbone

dihedral angles of protein residues. These angles were plotted to distinguish between favorable and unfavorable regions. The considerable model of RASSF3 was selected based on these graphical evaluations (**Fig. 1**) and 3D structure of RASSF3 was then visualized (**Fig. 2**).

Further evaluation of the predicted model was also performed. These plots display the distributions of φ and ψ angles specifically for non-glycine and non-proline residues (**Fig. 3**). The Ramachandran analysis helped differentiate between the favorable, allowed, and disallowed regions, thus aiding in assessing the stereochemical quality of the model.

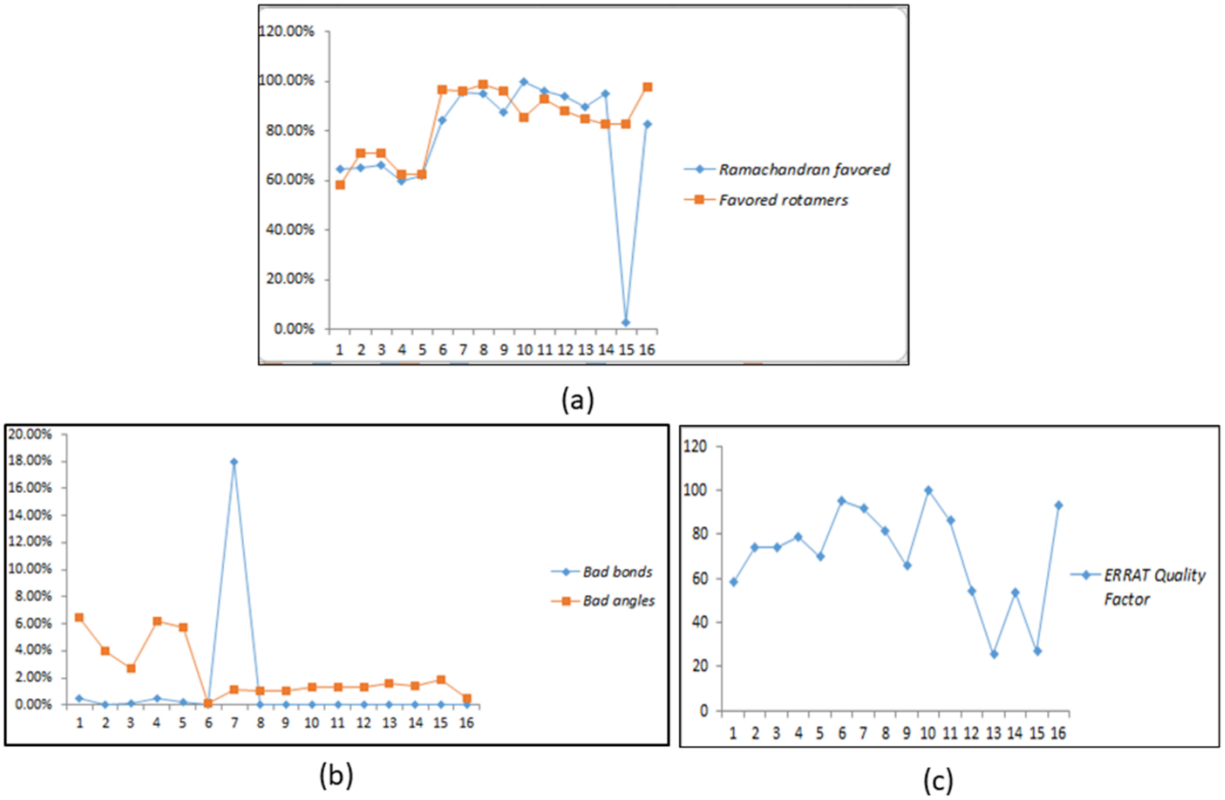

Fig. 1: (a) Favored regions are shown in blue, and favored rotamers are highlighted in brown. (b) Bad bonds are indicated in blue, while bad angles are marked in brown. (c) Overall quality factor of the predicted models.

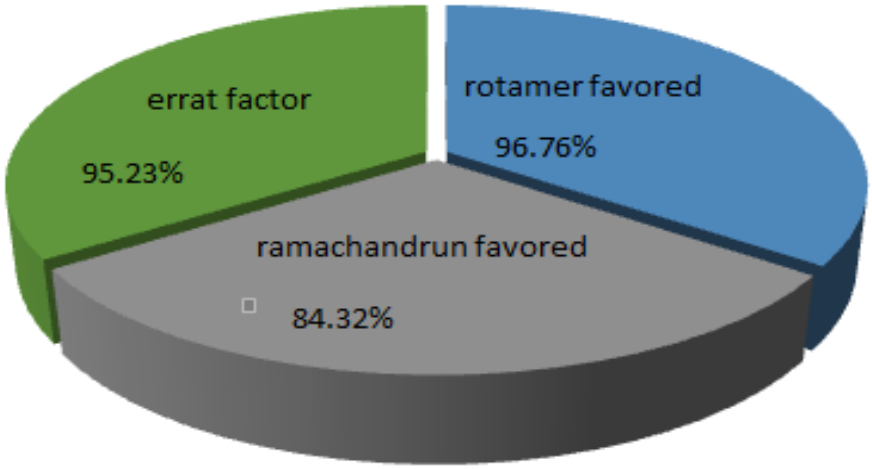

Fig. 2: Pie chart illustrating the contribution of structural validation parameters in the selected RASSF3 model. Overall quality factor is represented in green (95.24%), rotamer favored regions in blue (96.76%), and Ramachandran favored regions in grey (84.32%).

The modeled protein structure was evaluated for Ramachandran plot. The structure was evaluated for favored, allowed, and disallowed regions based on their φ (phi) and ψ (psi) angle distributions.

Residues located in disallowed regions should be remodeled, and the overall energy of the model minimized to improve stereochemical quality reducing the number of bad bonds and bond angles enhances structural reliability. The structural integrity of the model based on the density of residues in well-defined conformational regions were evaluated. The PDB-format structure of RASSF3 was submitted to PROCHECK, which identified and categorized the distribution of residues across favored, allowed, and disallowed regions (**Fig. 4**).

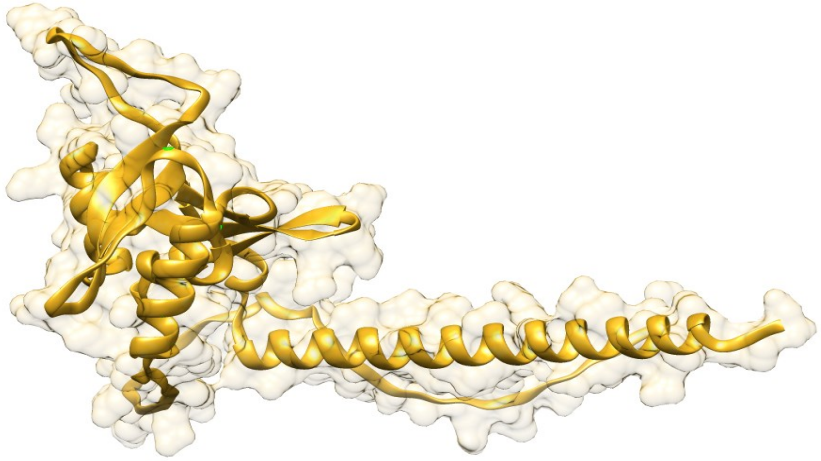

Fig. 3: 3D structure of RASSF3 selected based on structural evaluation metrics. The model shows α-helices formed by hydrogen bonding between the carbonyl group of one amino acid and the amide (N-H) group of another. In the β-pleated sheets, two polypeptide chains are aligned and stabilized by inter-chain hydrogen bonds.

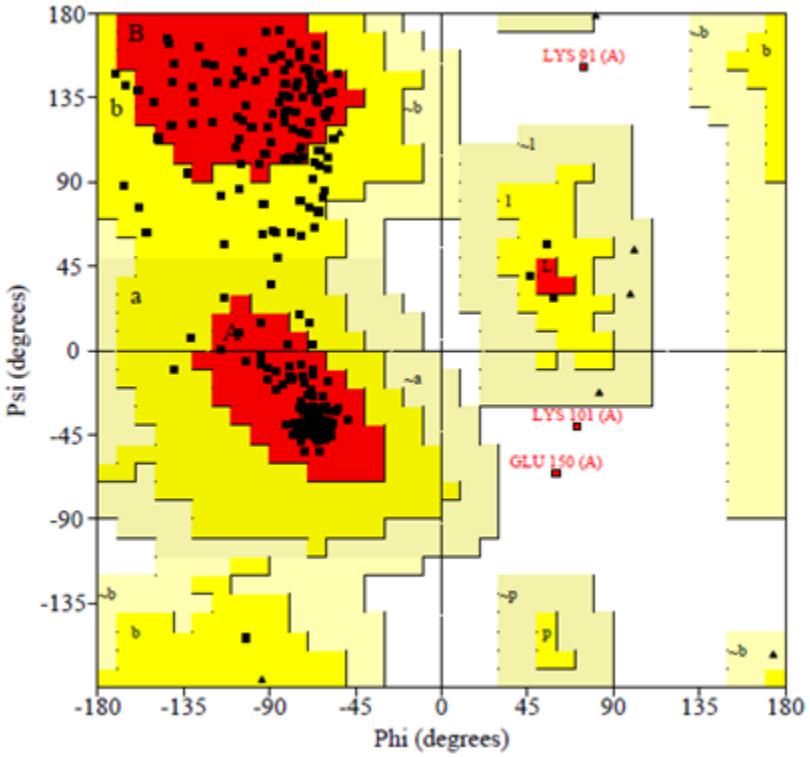

Fig. 4: Ramachandran plot showing the distribution of residues in the favored, allowed, and disallowed regions. The majority of residues were successfully located in the favored region, and only 3 residues were observed in the disallowed region.

Two reference lines were drawn on the error axis to indicate the confidence threshold for rejecting regions that exceed the acceptable error value. Overall quality score was expressed as the percentage of the protein model for which the calculated error value falls below the 95% rejection limit. High-resolution protein structures typically yield quality factor values above 95% (**Fig. 5**).

The top ten binding pockets of RASSF3 were identified and ranked based on their binding energy values (**Table 2**). Since the binding pockets of RASSF3 have not been previously reported, *in silico* approaches were employed to predict the potential target sites. The energy range of these predicted pockets reflects the strength of residue-residue interactions between the ligand and the receptor cavity.

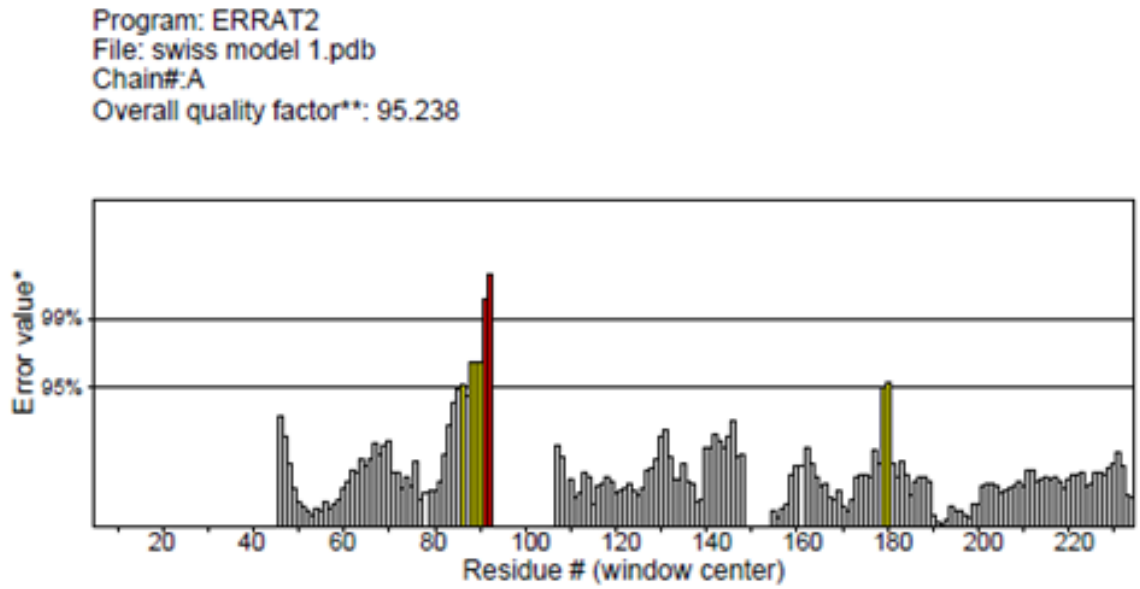

Fig. 5: Overall quality factor of the selected RASSF3 model, showing a score of 95.238%, indicating a high level of structural accuracy.

Table 2: Top ten predicted binding pockets of RASSF3, ranked by binding energy and cavity volume

Rank	Energy (kcal/mol)	Volume (Å)	Residues
1	-800.12	65.00	Phe-16, Phe-17, Arg-20, Thr-21, Lys-57, Lys-60, Tyr-61, Ala-64, Leu-169, Val-170, Ala-171, Gly-172, Pro-173, Arg-174
2	-588.63	43.00	Phe-24, Gly-30, Lys-31, Arg-33, Lys-41, Glu-42, Lys-145, Cys-147, Arg-149, Leu-167, Val-170, Ala-171, Leu-178
3	-559.05	51.00	Glu-88, Leu-89, Cys-90, Ser-106, Tyr-144, Arg-146, Val-181, Arg-183, Leu-205, Glu-208, Glu-211, Gln-212
4	-446.40	39.00	His-46, Leu-49, Ser-50, Lys-51, Ile-54, Asn-76, Gly-77, Ile-78, Ser-117, Thr-118, Tyr-166
5	-368.15	32.00	Asp-14, Phe-16, Phe-17, Asn-62, Leu-63, Ala-64, Val-65, Thr-66, Asp-67, Lys-70
6	-328.60	29.00	Arg-33, Ser-34, Asp-38, Val-39, Glu-42, Tyr-154, Cys-156, Leu-198, Gln-199
7	-328.25	31.00	Asn-62, Asp-67, Lys-70, Met-71, Thr-72, Thr-80, Gly-81, Phe-82, His-114
8	-315.93	27.00	Leu-129, Lys-130, Leu-133, Val-134, Thr-135, Glu-136, Pro-138
9	-275.45	25.00	Gly-122, Ile-125, Pro-138, Ala-139, Phe-141, Lys-157, Asp-160, Trp-190
10	-274.84	23.00	Arg-146, Gln-152, Val-153, Tyr-154, Ala-155, Leu-205, Asp-206, Glu-209

RASSF3 is a novel tumor suppressor gene that plays a critical role in inducing apoptosis during the early stages of cancer progression[39]. It is involved in the Hippo signaling pathway, which regulates cell proliferation and apoptosis. Deregulation of the Hippo pathway has been strongly associated with tumor development. Activation of the core kinases MST1/2 is essential for the proper functioning of this pathway. MST1/2 kinases, along with the SARAH domain, undergo both homodimerization and heterodimerization, leading to their activation at the activation loop[40]. The ligands ANP and GNP (**Fig. 6**) may contribute to the regulation or activation of the Hippo signaling pathway, potentially resulting in the inhibition of cancer.

Currently, there is no direct evidence of a specific regulator of RASSF3 activity within the signaling pathway, as observed in the case of RASSF2. Therefore, in this study, *in silico* techniques were employed to target RASSF3 in order to validate its binding pockets and identify potential regulators, similar to those reported for RASSF5 and RASSF2. Molecular docking was performed to predict the most favorable interactions between the selected ligands (ANP and GNP) and the RASSF3 protein.

The identification of binding pockets plays a crucial role in drug discovery, particularly in the development of anti-cancer therapeutics. Molecular docking was carried out using AutoDock Vina and AutoDock4 [41], employing the same compounds in both tools for comparative analysis. The resulting docked complexes were ranked based on their lowest binding energy. Prior to docking, energy minimization of the ligands ANP and GNP was conducted.

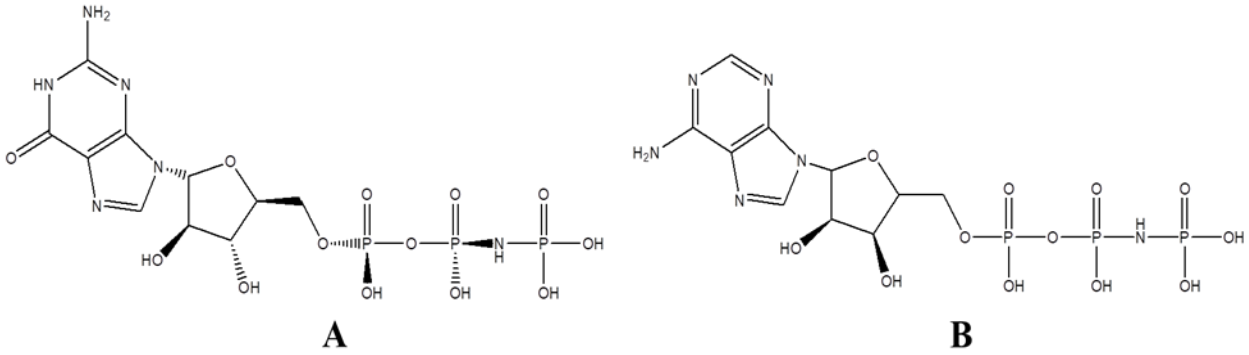

Fig. 6: 2D structures of selected ligands: **A)** Phosphoaminophonic acid acetylate ester (ANP) and **B)** Phosphoaminophonic acid guanylate ester (GNP)

Table 3: RASSF3 residues involved in interactions with ligands ANP and GNP, along with their corresponding binding energies

Ligands	Binding Energy (kcal/mol)	Residues
ANP	-5.2	Tyr-61, Ala-64, Pro-173, Phe-17, Lys-60, Leu-169, Gly-172, Lys-57, Thr-21, Val-170, Arg-20, Glu-44, Ala-19
GNP	-5.7	Tyr-61, Ala-64, Pro-173, Phe-17, Lys-60, Leu-169, Gly-172, Lys-57, Thr-21, Val-170, Arg-20, Glu-44, Ala-171, Phe-17, Arg-174

Based on the number of interactions between the ligands (ANP and GNP) and the target receptor (RASSF3), both AutoDock4 and AutoDock Vina predicted binding within a similar binding pocket. The interacting residues were analyzed and visualized. Notably, both ANP and GNP exhibited the lowest binding energies and the highest binding affinities within the top-ranked binding pocket of RASSF3 (**Table 3**).

The specific interactions between RASSF3 and the ligands were further analyzed and visualized. The docking results confirmed that ANP and GNP bind within the same predicted binding site, interacting with key residues including Tyr-61, Ala-64, Pro-173, Phe-17, Lys-60, Leu-169, Gly-172, Lys-57, Thr-21, Val-170, Arg-20, and Glu-44 (**Figs. 7-10**).

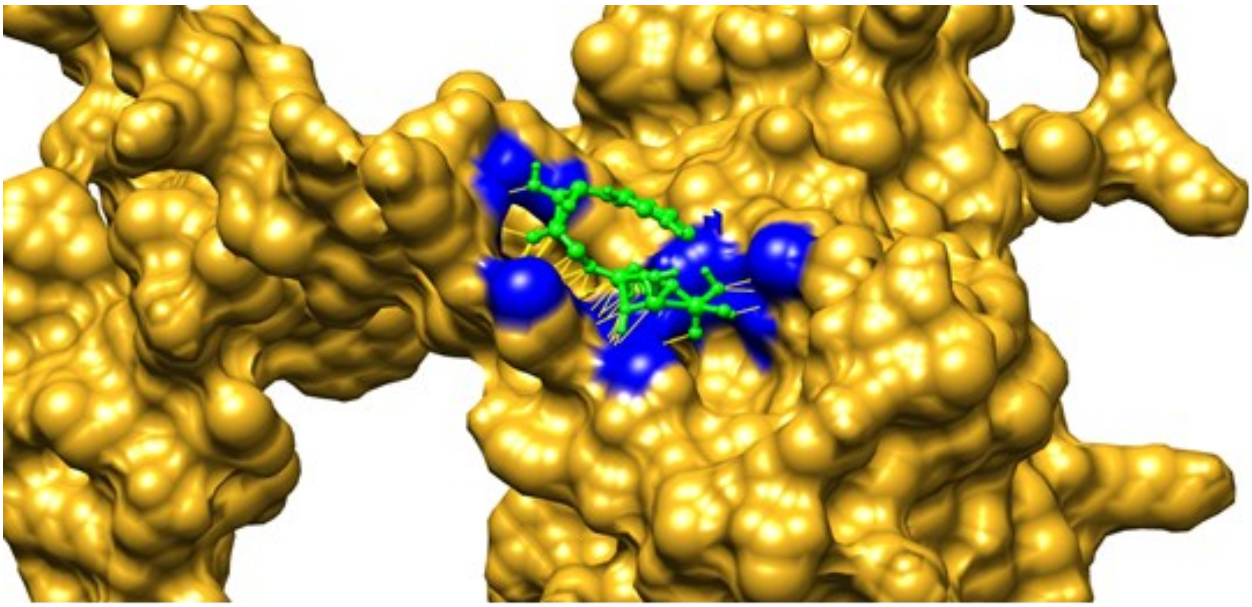

Fig. 7: Binding interaction between RASSF3 and the ligand ANP. The active binding cavity is highlighted in blue, while the docked ligand ANP is shown in green

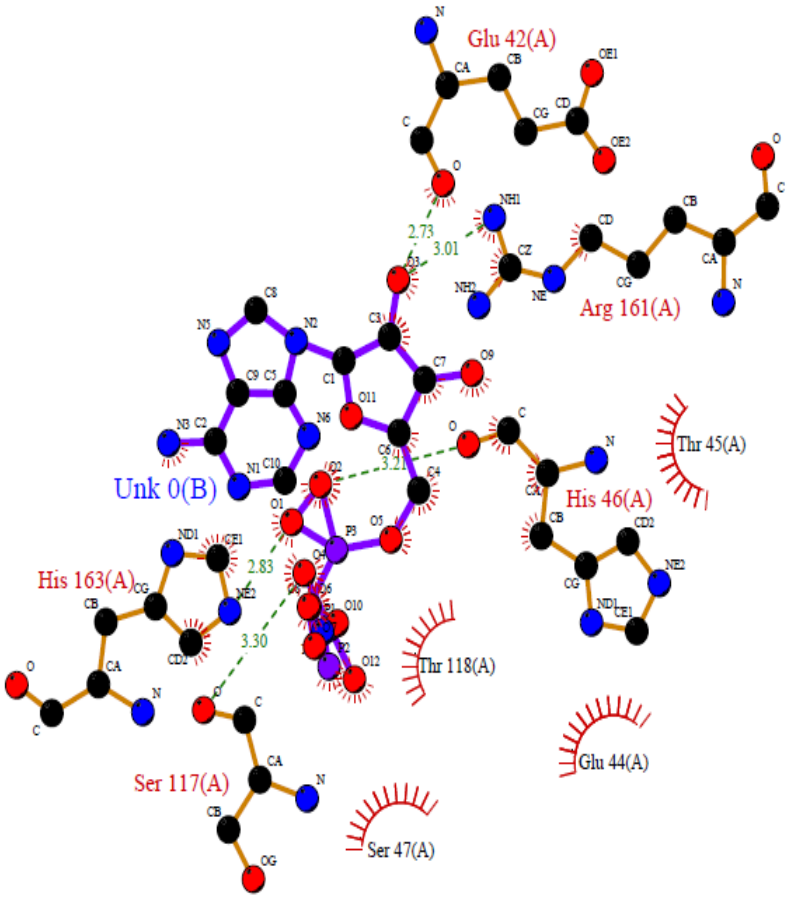

Fig. 8: Visualization of the interaction between RASSF3 and the ligand ANP. Interacting residues are indicated by red dotted lines, while hydrogen bonds are shown as blue dotted lines.

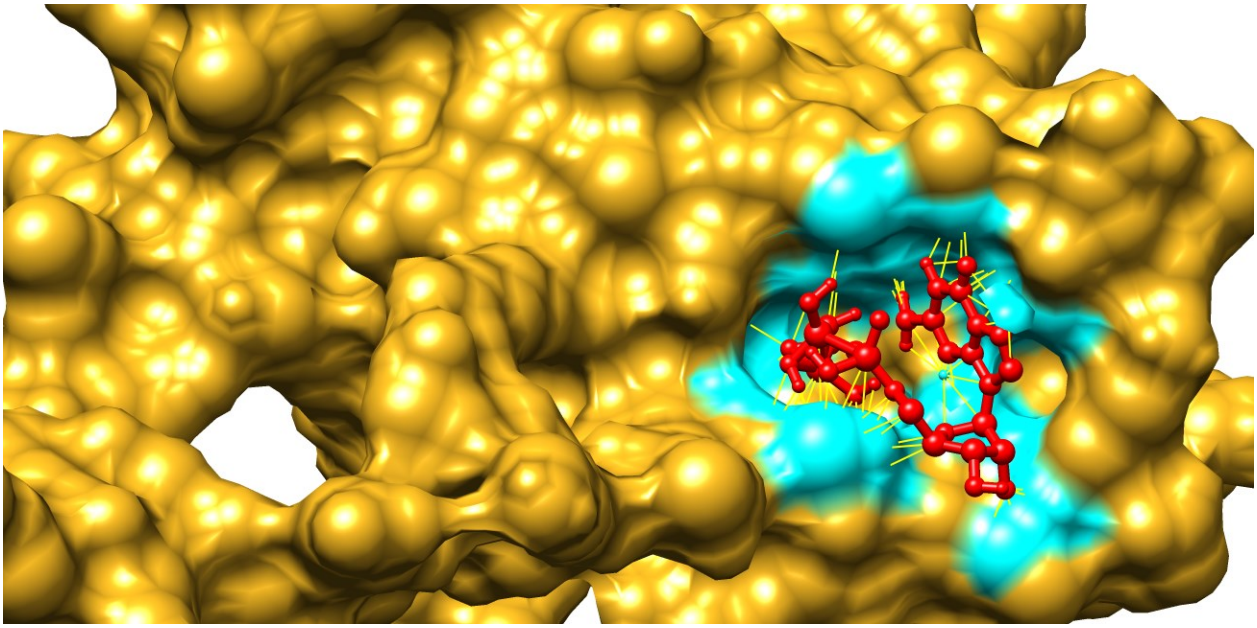

Fig. 9: Binding interaction between RASSF3 and the ligand GNP. The active binding cavity where GNP is docked is shown in cyan, while the ligand GNP is displayed in red.

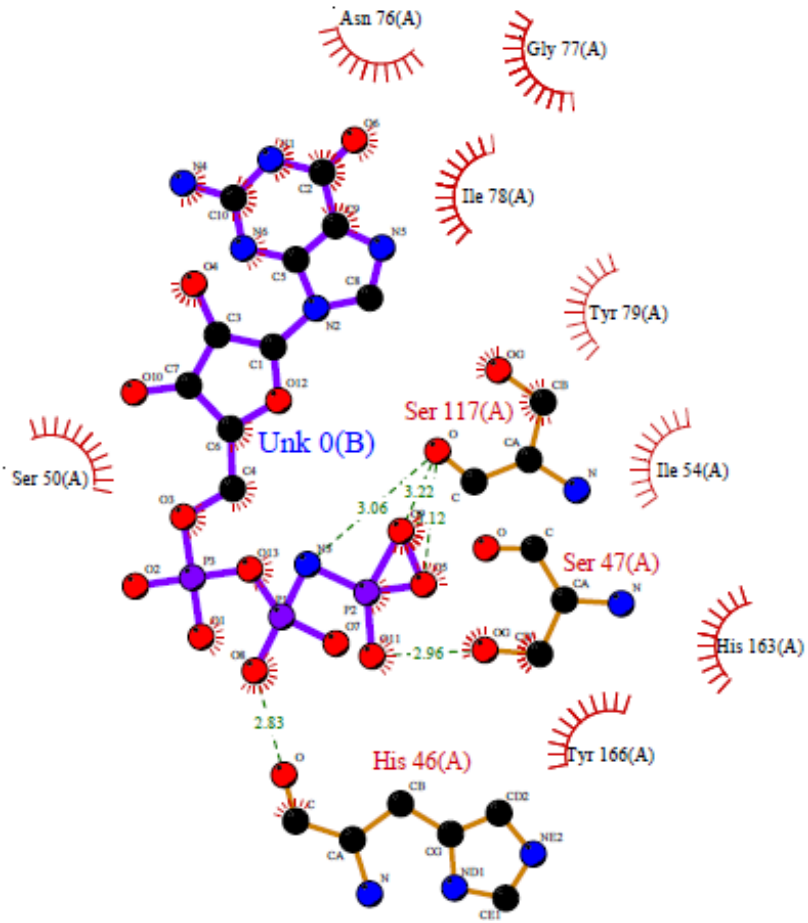

Fig. 10: Visualization of the interaction between RASSF3 and the ligand GNP. Interacting residues are represented by red dotted lines, while hydrogen bonds are shown as blue dotted lines.

The field of bioinformatics plays a significant role in cancer treatment [42], [43], [44], as traditional drug discovery methods are often costly and time-consuming. As a result, *in silico* approaches have become increasingly valuable for designing potential anticancer agents [45, 46]. Protein function is inherently dependent on its structure; thus, effective drug design requires knowledge of the protein's 3D structure and active binding domains. In this study, *in silico* techniques were employed to predict the 3D structure and identify the binding domains of the tumor suppressor protein RASSF3. These findings may facilitate the development of targeted cancer therapies by providing structural insights essential for rational drug design. The selected compounds, ANP and GNP, demonstrated strong binding affinity to RASSF3 during molecular docking analysis, potentially enhancing the functional activity of RASSF3 in suppressing tumor progression.

Conclusion

In this study, 3D model of the RASSF3 protein was successfully predicted using multiple modeling approaches and validated through structural evaluation tools to select the most reliable model. The top ten binding pockets of RASSF3 were identified and ranked based on their binding energies. These findings highlight the potential of RASSF3 as a target in cancer research. The predicted protein structure may further serve as a framework for exploring interactions with other cancer-related proteins. Molecular docking analyses revealed that the selected compounds, ANP and GNP, exhibit strong binding affinity to the predicted active sites of RASSF3, suggesting their potential role in regulating its activity. These compounds may serve as lead candidates for further studies targeting the RASSF protein family. Their successful docking into RASSF3's binding sites indicates promising potential for drug delivery to specific target sites in cancer therapy.

Conflict of interest

The authors declare no conflict of interest.

References

[1] Keyvani V, Kerachian MA. The effect of fasting on the important molecular mechanisms related to cancer treatment. 2014.

[2] Berliner JL, Fay AM, Cummings SA, Burnett B, Tillmanns T. NSGC practice guideline: risk assessment and genetic counseling for hereditary breast and ovarian cancer. Journal of genetic counseling. 2013;22:155-63.

[3] Kanwal S, Jamil F, Ali A, Sehgal SA. Comparative modeling, molecular docking, and revealing of potential binding pockets of RASSF2; a candidate cancer gene. Interdisciplinary Sciences: Computational Life Sciences. 2017;9:214-23.

[4] Hanahan D, Weinberg RA. The hallmarks of cancer. cell. 2000;100:57-70.

[5] Knudson AG. Two genetic hits (more or less) to cancer. Nature Reviews Cancer. 2001;1:157-62.

[6] Mao L, Hong WK, Papadimitrakopoulou VA. Focus on head and neck cancer. Cancer cell. 2004;5:311-6.

[7] Leemans CR, Braakhuis BJ, Brakenhoff RH. The molecular biology of head and neck cancer. Nature reviews cancer. 2011;11:9-22.

[8] Icard P, Lincet H. A global view of the biochemical pathways involved in the regulation of the metabolism of cancer cells. Biochimica et Biophysica Acta (BBA)-Reviews on Cancer. 2012;1826:423-33.

[9] Hong WK, Sporn MB. Recent advances in chemoprevention of cancer. Science. 1997;278:1073-7.

[10] Hesson LB, Dunwell TL, Cooper WN, Catchpoole D, Brini AT, Chiaramonte R, et al. The novel RASSF6 and RASSF10 candidate tumour suppressor genes are frequently epigenetically inactivated in childhood leukaemias. Molecular cancer. 2009;8:42.

[11] Pfeifer GP, Dammann R, Tommasi S. RASSF proteins. Current Biology. 2010;20:R344-R5.

[12] Hesson LB, Cooper WN, Latif F. The role of RASSF1A methylation in cancer. Disease markers. 2007;23:73-87.

[13] Tommasi S, Dammann R, Jin S-G, Zhang X-f, Avruch J, Pfeifer GP. RASSF3 and NORE1: identification and cloning of two human homologues of the putative tumor suppressor gene RASSF1. Oncogene. 2002;21:2713-20.

[14] Menashe I, Maeder D, Garcia-Closas M, Figueroa JD, Bhattacharjee S, Rotunno M, et al. Pathway analysis of breast cancer genome-wide association study highlights three pathways and one canonical signaling cascade. Cancer research. 2010;70:4453-9.

[15] Jacquemart IC, Springs AE, Chen WY. Rassf3 is responsible in part for resistance to mammary tumor development in neu transgenic mice. International journal of oncology. 2009;34:517-28.

[16] Guo H, Liu H, Wei J, Li Y, Yu H, Guan X, et al. Functional single nucleotide polymorphisms of the RASSF3 gene and susceptibility to squamous cell carcinoma of the head and neck. European Journal of Cancer. 2014;50:582-92.

[17] Jin Y, Sehgal SA, Hassan F, Liu G. In Silico Identification of Novel Compounds as Anthelmintics Against Haemonchus contortus Through Inhibiting β-Tubulin Isotype 1 and Glutathione S-Transferase. Animals. 2025;15:1846.

[18] Sehgal SA, Razia IT, Kanwal A, Ahsan M, Tahir RA, Sajid M, et al. Computational Advancement towards the Identification of Natural Inhibitors for Dengue Virus: A Brief Review. Combinatorial Chemistry and High Throughput Screening. 2024;26.

[19] Sehgal SA, Khattak NA, Mir A. Structural, phylogenetic and docking studies of D-amino acid oxidase activator (DAOA), a candidate schizophrenia gene. Theoretical Biology and Medical Modelling. 2013;10:3.

[20] Sehgal SA, Hassan M, Rashid S. Pharmacoinformatics elucidation of potential drug targets against migraine to

target ion channel protein KCNK18. Drug design, development and therapy. 2014:571-81.
[21] Tahir RA, Bashir A, Yousaf MN, Ahmed A, Dali Y, Khan S, et al. In Silico identification of angiotensin-converting enzyme inhibitory peptides from MRJP1. PloS one. 2020;15:e0228265.
[22] Marriam S, Afghan MS, Nadeem M, Sajid M, Ahsan M, Basit A, et al. Elucidation of novel compounds and epitope-based peptide vaccine design against C30 endopeptidase regions of SARS-CoV-2 using immunoinformatics approaches. Frontiers in Cellular and Infection Microbiology. 2023;13:1134802.
[23] Consortium U. UniProt: a hub for protein information. Nucleic acids research. 2015;43:D204-D12.
[24] Burley SK, Berman HM, Kleywegt GJ, Markley JL, Nakamura H, Velankar S. Protein Data Bank (PDB): the single global macromolecular structure archive. Protein crystallography: methods and protocols. 2017:627-41.
[25] Pettersen EF, Goddard TD, Huang CC, Couch GS, Greenblatt DM, Meng EC, et al. UCSF Chimera-A visualization system for exploratory research and analysis. Journal of computational chemistry. 2004;25:1605-12.
[26] Zhang Y. I-TASSER server for protein 3D structure prediction. BMC bioinformatics. 2008;9:40.
[27] Schwede T, Kopp J, Guex N, Peitsch MC. SWISS-MODEL: an automated protein homology-modeling server. Nucleic acids research. 2003;31:3381-5.
[28] Eswar N, John B, Mirkovic N, Fiser A, Ilyin VA, Pieper U, et al. Tools for comparative protein structure modeling and analysis. Nucleic acids research. 2003;31:3375-80.
[29] Aronson E. The jigsaw classroom: Sage; 1978.
[30] Webb B, Sali A. Comparative protein structure modeling using MODELLER. Current protocols in bioinformatics. 2016;54:5.6. 1-5.6. 37.
[31] Chen VB, Arendall WB, Headd JJ, Keedy DA, Immormino RM, Kapral GJ, et al. MolProbity: all-atom structure validation for macromolecular crystallography. Biological crystallography. 2010;66:12-21.
[32] Dym O, Eisenberg D, Yeates T. Examples: detection of errors in structures. 2006.
[33] Laskowski RA, MacArthur MW, Moss DS, Thornton JM. PROCHECK: a program to check the stereochemical quality of protein structures. Applied Crystallography. 1993;26:283-91.
[34] Lohkamp B, Emsley P, Cowtan K. Coot news. CCP4 Newsletter. 2005;42:3-5.
[35] Tian W, Chen C, Lei X, Zhao J, Liang J. CASTp 3.0: computed atlas of surface topography of proteins. Nucleic acids research. 2018;46:W363-W7.
[36] Li Z, Wan H, Shi Y, Ouyang P. Personal experience with four kinds of chemical structure drawing software: review on ChemDraw, ChemWindow, ISIS/Draw, and ChemSketch. Journal of chemical information and computer sciences. 2004;44:1886-90.
[37] Eberhardt J, Santos-Martins D, Tillack AF, Forli S. AutoDock Vina 1.2. 0: new docking methods, expanded force field, and python bindings. Journal of chemical information and modeling. 2021;61:3891-8.
[38] Sehgal SA, Tahir RA, Waqas M. Quick Guideline for Computational Drug Design (Revised Edition): Bentham Science Publishers; 2021.
[39] Akino K, Toyota M, Suzuki H, Mita H, Sasaki Y, Ohe-Toyota M, et al. The Ras effector RASSF2 is a novel tumor-suppressor gene in human colorectal cancer. Gastroenterology. 2005;129:156-69.
[40] Ni L, Li S, Yu J, Min J, Brautigam CA, Tomchick DR, et al. Structural basis for autoactivation of human Mst2 kinase and its regulation by RASSF5. Structure. 2013;21:1757-68.
[41] Morris GM, Huey R, Lindstrom W, Sanner MF, Belew RK, Goodsell DS, et al. AutoDock4 and AutoDockTools4: Automated docking with selective receptor flexibility. Journal of computational chemistry. 2009;30:2785-91.
[42] Waseem HB, Shakeel M, Hassan F-U, Yaqoob A, Iqbal A, Khalid A, et al. In silico Identification and Computational Screening of Potential AFP Inhibitors Against Liver Cancer. Medicinal chemistry (Shariqah (United Arab Emirates)). 2025.
[43] Tur Razia I, Kanwal A, Riaz HF, Malik A, Ahsan M, Saleem Khan M, et al. Recent trends in computer-aided drug design for anti-cancer drug discovery. Current Topics in Medicinal Chemistry. 2023;23:2844-62.
[44] Sehgal SA, Kanwal S, Tahir RA, Khalid Z, Hammad MA. In silico elucidation of potential drug target sites of the Thumb Index Fold Protein, Wnt-8b. Tropical Journal of Pharmaceutical Research. 2018;17:491-7.
[45] Tahir RA, Sehgal SA, Khattak NA, Khan Khattak JZ, Mir A. Tumor necrosis factor receptor superfamily 10B (TNFRSF10B): an insight from structure modeling to virtual screening for designing drug against head and neck cancer. Theoretical Biology and Medical Modelling. 2013;10:38.
[46] Sehgal S, Tahir R, Shafique S, Hassan M, Rashid S. Molecular modeling and docking analysis of CYP1A1 associated with head and neck cancer to explore its binding regions. J Theor Comput Sci. 2014;1:2.